

PAPER

Superharmonic vibration and its reduction in SSD control by increase of voltage inversion time

To cite this article: Hongli Ji *et al* 2018 *Smart Mater. Struct.* **27** 085007

View the [article online](#) for updates and enhancements.

Related content

- [The influence of switching phase and frequency of voltage on the vibration damping effect in a piezoelectric actuator](#)
Hongli Ji, Jinhao Qiu, Pinqi Xia et al.
- [Energy conversion and performance of switched-voltage control based on negative capacitance with arbitrary switching frequency](#)
Hongli Ji, Jinhao Qiu, Pinqi Xia et al.
- [Coupling analysis of energy conversion in multi-mode vibration structural control using a synchronized switch damping method](#)
Hongli Ji, Jinhao Qiu, Pinqi Xia et al.

Superharmonic vibration and its reduction in SSD control by increase of voltage inversion time

Hongli Ji¹ , Zining Chen², Jinhao Qiu^{1,4}, Yipeng Wu^{1,4}  and Li Cheng³ 

¹ State Key Laboratory of Mechanics and Control of Mechanical Structures, Nanjing University of Aeronautics and Astronautics, Nanjing 210016, People's Republic of China

² Sino-French Engineer School, Nanjing University of Science and Technology, Nanjing 210094, People's Republic of China

³ Department of Mechanical Engineering, Hong Kong Polytechnic University, Hung Hom, Kowloon, Hong Kong

E-mail: qiu@nuaa.edu.cn and yipeng.wu@nuaa.edu.cn

Received 10 April 2018, revised 28 May 2018

Accepted for publication 20 June 2018

Published 10 July 2018



CrossMark

Abstract

The semi-active synchronized switch damping (SSD) approach has been widely used in vibration suppression owing to its many advantages compared with the active and passive approaches. The SSD method is realized by switching the voltage on the piezoelectric patch embedded in the structure, synchronically with the vibration of the mode to be controlled. Although good control performance can be obtained in the targeted mode, vibrations of high-order harmonic frequencies are usually excited due to the rectangular waveform of the switched actuator voltage because of infinitesimal inversion time, as observed in the previous experiments. This drawback of the SSD method has greatly hindered its application in practical engineering structures. In order to overcome this drawback, the authors propose a new method in this study to suppress the high-order harmonic components in the switched voltage by increasing the inversion time of the voltage. The theoretical expressions of the switched voltage and the dynamic response of the structure were formulated for the cases with finite voltage inversion time. The theoretical results show that increasing the inversion time may weaken the vibration control effect of the targeted mode, but it can significantly reduce the excitation force of the high-order harmonic components. When the inversion time is half of the period of the targeted mode, all the high-order harmonic components in the actuator voltage are completely erased and the control force of the targeted mode decreases by 21%. An experimental setup of a flexible beam was used to verify the theoretical results of the switched voltage and control performance under different inversion time.

Keywords: semi-active vibration control, piezoelectric elements, synchronized switch damping, superharmonic vibration

(Some figures may appear in colour only in the online journal)

1. Introduction

Developing high-performance, light-weight and low-power vibration and noise control systems is of great importance in order to solve various engineering problems, especially for

the aerospace industry [1–6]. The semi-active synchronized switch damping (SSD) approach using piezoelectric actuators as one of the methods of vibration control was first proposed by Richard *et al* in 1998 [3]. In the semi-active switched-voltage control, the switch circuit is composed of an inductor L and the switch is connected in series with the piezoelectric element. The switch is closed at the displacement or strain

⁴ Authors to whom any correspondence should be addressed.

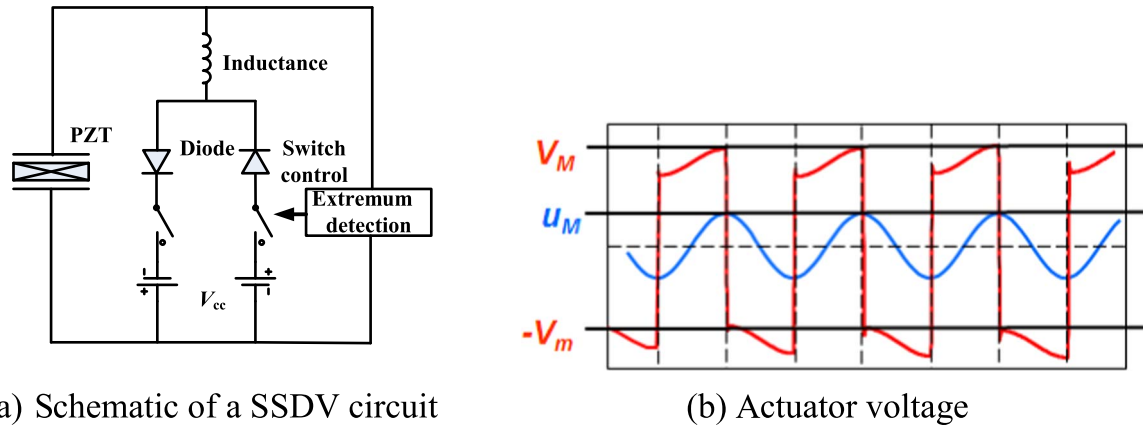


Figure 1. Principle of SSDV.

extremes. Because the piezoelectric patch and inductor constitute an LC resonance circuit, fast inversion of the voltage on the piezoelectric patch is achieved by appropriately controlling the closing time. Great magnification of the voltage amplitude is then obtained and a quadrature phase is observed between the voltage and displacement, thus leading to an artificial increase of the dissipated energy.

The SSD method shows appealing features in vibration control because no proportional power amplifiers and high-performance digital signal processing units are required, so these systems are much easier to implement for practical applications. Apart from simplicity of the system, the power consumed by an SSD control system is usually very low due to fast inversion of the voltage on the piezoelectric actuators by a resonant shunt circuit. The SSD method shows its great potential in vibration control because of several advantages. Recently, a number of investigations have been carried out with the aim of improving the control performance using the SSD method [4–18].

Several variances of the SSD method, including synchronized switch damping on inductor (SSDI) [19], synchronized switch damping on voltage source (SSDV) [20, 21], adaptive SSDV [22–24], and SSD based on negative capacitor (SSDNC) have been developed in the past ten years [25–27]. Since the switching phase and switching frequency are factors critical to damping performance in the SSD method, their influence on converted energy has been investigated rigorously [28]. Many switching control algorithms have been developed to maximize the energy dissipated in each cycle of vibration [29–31].

In SSDI and SSDV the switch circuit is inductive and in SSDNC the switch is capacitive. In either case, the switch circuit is used to invert the voltage on the piezoelectric actuator very quickly at the displacement extrema to obtain maximum control performance. Figure 1(a) is a typical circuit of SSDV and figure 1(b) is the typical waveform of voltage on the piezoelectric actuator. Obviously, the duration of voltage inversion is much shorter than the period of mechanical vibration, with their ratio ranging from 1/20 and 1/50. Therefore, it was usually assumed in the previous studies that the voltage was inverted instantaneously.

The voltage $V_a(t)$ on the piezoelectric element in the steady state of SSD control can be decomposed into two parts: V_{st} , the voltage induced by mechanical strain, and V_{sw} , the voltage due to switching action [28]. Hence, the actuator voltage can be expressed in the following form:

$$V_a(t) = V_{st}(t) + V_{sw}(t). \quad (1)$$

Since it is assumed that the actuator voltage is inverted in infinitesimal time, the voltage V_{sw} is a rectangular function with the same frequency as the mechanical vibration. Consequently, in addition to the fundamental harmonic component used to suppress the targeted vibration, the voltage V_{sw} also contains high-order harmonic components, which excite additional vibration at these superharmonic frequencies. This is the main drawback of SSD control, which hinders its even wider application, especially in noise reduction [32].

In this study, a method is proposed to overcome the drawback of SSD control so that the switched voltage with a rectangular waveform excites superharmonic vibrations, by increasing the inversion time of the voltage. A systematic investigation on the influence of the inversion time on both fundamental harmonic and superharmonic components of the switch voltage, which directly affect the control performance of the targeted mode and excited superharmonic vibration, is presented. The paper is organized as follows. In section 2, the electromechanical model of the SSD system is presented and general expressions of the switched voltage on the piezoelectric actuator under non-resonance excitation without considering the inversion time are derived. The displacement response of the dominant mode is also solved under combined actions of the excitation and switched voltage. And then, the superharmonic vibration induced by the switched actuator voltage is obtained. In section 3, the reduction of superharmonic components by increasing the voltage inversion time is proposed and the switched voltage considering the inversion time is analyzed using Fourier series. The damping effect of the fundamental harmonic of the first mode and superharmonic vibration are also given in section 3. In section 4, an experiment of a stiff beam with SSDV control was used to demonstrate the application of the theoretical results. The theoretical and experimental results show that the sharpness of the converted voltage on PZT can be reduced by increasing the

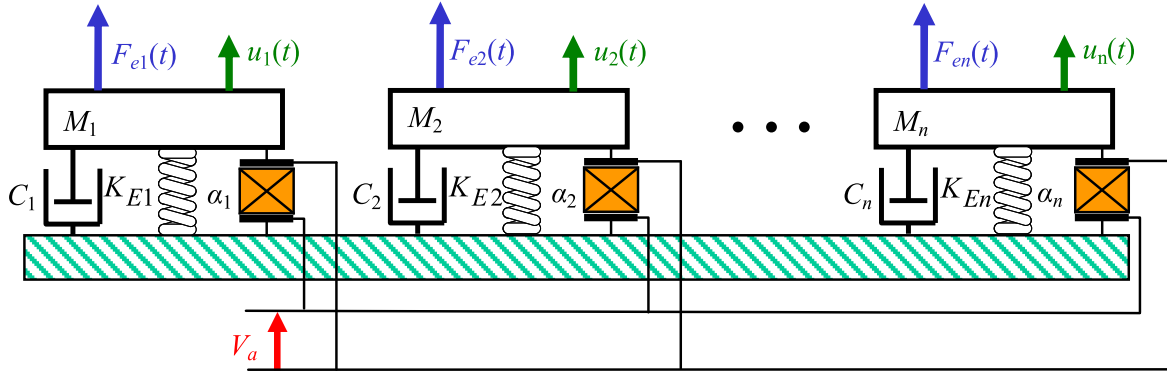


Figure 2. Diagram of the multimode electromechanical model.

voltage inversion time. The fundamental harmonic voltage component is not decreased significantly as the increasing of the inversion time, but the high-order harmonic voltage components can be reduced effectively. The phenomenon is especially important for the application of SSD control in the engineering field. Conclusions are drawn in section 5.

2. Superharmonic vibration in SSD control with infinitesimal inversion time of shunt circuit

2.1. General electromechanical model of a vibration system

A continuous structure can be modeled as a multi-degree-of-freedom system after modal truncation [26, 28]. Although the switching actions can lead to modal coupling, this kind of coupling is weak and can be ignored in analysis [33]. Hence, it is assumed in the following analysis that the modal displacements are uncoupled and the superposition principle can be applied. The total displacement u can be expressed in the following form:

$$u = \sum_{i=1}^N u_i, \quad (2)$$

where u_i is the modal displacement of i th mode and N is the total number of modes considered.

The electromechanical model of the system, shown in figure 2, was proposed in [28, 33] and is included in this paper for easy reference to readers. This model gives a good description of the vibrating behavior of a structure in the low-frequency

where M_i represents the modal mass, C_i is the modal damping coefficient due to inherent structural viscoelasticity, K_{Ei} is the modal stiffness of the structural system, which can be expressed as

$$K_{Ei} = K_{Si} + K_i^{sc}, \quad (4)$$

where K_{Si} is the stiffness of the host structure and the K_i^{sc} is the stiffness of the piezoelectric transducer in short circuit. The terms on the right-hand side of equation (3) represent the modal forces acting on the modal mass, including the force due to excitation, F_{ei} , and the force generated by the piezoelectric elements, F_{ci} , which is described by

$$F_{ci} = -\alpha_i V_a, \quad (5)$$

where V_a is the voltage on the piezoelectric elements, α_i is the force factor.

In the case of harmonic, the excitation and response can be assumed to have the following form:

$$F_{ei} = F_{Mi} \sin \omega_e t, \quad u_i(t) = u_{Mi} \sin(\omega_e t - \varphi_{ui}), \quad (6)$$

where F_{Mi} is the amplitude of the excitation force, ω_e is the angular frequency of excitation, which may not be equal to the angular natural frequency of the system, ω_{ni} . φ_{ui} is the phase delay of the displacement with respect to the excitation force.

After equation (6) is substituted into equation (3), the amplitude and phase of vibration without control can be expressed in the following form:

$$\begin{cases} u_{Mi} = \frac{F_{Mi}}{\sqrt{(K_{Ei} - M_i \omega_e^2)^2 + (C_i \omega_e)^2}} = \frac{F_{Mi}/K_{Ei}}{\sqrt{\left(1 - \left(\frac{\omega_e}{\omega_{ni}}\right)^2\right)^2 + \left(2\zeta_i \left(\frac{\omega_e}{\omega_{ni}}\right)\right)^2}}, \\ \tan \varphi_{ui} = \frac{C_i \omega_e}{K_{Ei} - M_i \omega_e^2} = \frac{2\zeta_i \omega_e / \omega_{ni}}{1 - (\omega_e / \omega_{ni})^2} \end{cases}, \quad (7)$$

range. The governing equation of the i th mode is given by

$$M_i \ddot{u}_i + C_i \dot{u}_i + K_{Ei} u_i = F_{ei} + F_{ci}, \quad (3)$$

where

$$\omega_{ni} = \sqrt{K_{Ei}/M_i}, \quad \zeta_i = C_i/2M_i\omega_{ni}, \quad (8)$$

are the natural frequency of undamped oscillation and the damping ratio, respectively. Obviously, if the excitation frequency satisfies $\omega_e = \omega_{ni}$, the phase delay is $\varphi_{ui} = \pi/2$.

2.2. Performance of SSD control under non-resonance excitation

In this section, the principle of SSD control is reviewed in order to study the effect of inversion time on switched voltage in this paper, with similar descriptions having been presented in earlier papers [28]. A typical switch circuit for the SSDV method has been shown in figure 1(a). If there were no voltage sources in the circuit, it becomes the switch circuit of SSDI control. Switches in the circuit are closed at every maximum or minimum of the displacement and are kept closed for half a period of the electrical oscillator, which results in the inversion of voltage, as shown in figure 1(b). Due to the switch control, the force generated by the voltage is always opposite to the velocity \dot{u} of the vibrating structure, thus creating net mechanical energy dissipation.

In the previous studies, it was always assumed that the structure was excited at one of the resonance frequencies. In this section, the response and control performance of a structure under non-resonance excitation and SSD control are discussed. Without loss of generality, the excitation frequency is assumed to be near to, but not at, the natural frequency of the first mode, in the following discussions, that is, $\omega_e \approx \omega_{n1}$. The vibration of the first mode is dominant and the other modes are only weakly excited, so that their modal displacements induced by the external excitation are negligible. It is also assumed that superharmonic components of the first mode due to switched voltage are also negligible, so that its displacement response can be expressed in the following form:

$$u_1(t) = u_{M1} \sin(\omega_e t - \varphi_{u1}). \quad (9)$$

In order to control this dominant mode, the displacement in equation (9) is used for switch control. That is, the voltage is inverted at the extrema of the displacement in the above equation, which means the switch is closed twice in each cycle of mechanical vibration. The switching frequency is twice the frequency of the mechanical vibration, which is defined as

$$\omega_{sw} = \frac{2\pi}{\tau_{sw}} = 2\omega_e. \quad (10)$$

τ_{sw} , defined as the switching period, is the time duration between two neighboring switching points.

The voltage $V_a(t)$ on the piezoelectric element in the steady state of SSD control is the sum of two parts, as shown in equation (1). The voltage V_{st} is generated by the strain due to vibration and can be approximately expressed as

$$V_{st}(t) = \sum_{i=1}^N \frac{\alpha_i}{C_p} u_i(t) \approx \frac{\alpha_1}{C_p} u_1(t), \quad (11)$$

because the first mode is dominant, where C_p is the inherent capacitance of the piezoelectric actuator.

In the previous studies, the switched voltage V_{sw} was always assumed to be rectangular wave because of very short voltage inversion time, which is half the period of the electrical oscillation in the LC switch circuit and is roughly between 1/20 and 1/50 of the period of mechanical vibration [22, 23]. Hence, the switched voltage can be expressed in the following form:

$$V_{sw}(t) = \hat{V}_{sw} S_{\tau_{sw}}(t), \quad (12)$$

where \hat{V}_{sw} is the amplitude of V_{sw} , $S_{\tau_{sw}}(t)$ is a switch function with a switching period of τ_{sw} . The switch function is defined as

$$S_{\tau_{sw}}(t) = \begin{cases} -1 & t_{2k-1} \leq t < t_{2k} \\ +1 & t_{2k} \leq t < t_{2k+1} \end{cases} \quad (k = 0, \pm 1, \pm 2, \dots). \quad (13)$$

According to the displacement of the first mode in equation (7), the phase delay can be expressed as

$$\varphi_{u1} = \pi/2 + \varphi'_{u1}, \quad (14)$$

in which $-\pi/2 < \varphi'_{u1} < \pi/2$. The switch points are

$$t_k = k\tau_{sw} + \frac{\varphi'_{u1}}{\omega_e} = k\frac{\pi}{\omega_e} + \frac{\varphi'_{u1}}{\omega_e} \quad (k = 0, \pm 1, \pm 2, \dots). \quad (15)$$

The switched actuator voltage is periodic and expanded in Fourier series. For convenience, the time is shifted by φ'_{u1}/ω_e and the new time t' is defined as $t' = t - \varphi'_{u1}/\omega_e$. Then, $V_{sw}(t')$ is an odd function and can be expressed in Fourier series as follows:

$$V_{sw}(t') = \sum_{k=1}^{\infty} b_k^{sw} \sin k \frac{\omega_{sw}}{2} t'. \quad (16)$$

The coefficient b_k^{sw} in equation (16) can be calculated as follows:

$$b_k^{sw} = \begin{cases} \frac{4}{(2j-1)\pi} \hat{V}_{sw} & (k = 2j-1, j = 1, 2, \dots) \\ 0 & (k = 2j, j = 1, 2, \dots) \end{cases}. \quad (17)$$

The above expression shows that due to the switching action, the actuator voltage contains the odd-order superharmonic components, and all the even-order components are zero.

In the SSDV control, the amplitude of switched voltage can be expressed in the following form [21]:

$$\hat{V}_{sw} = \frac{1 + \gamma}{1 - \gamma} \left(\frac{\alpha_1}{C_p} u_{M1} + V_{cc} \right), \quad (18)$$

where γ is the voltage inversion efficiency of the circuit and V_{cc} is the output of the voltage source. In the enhanced SSDV control, the output of the voltage source is assumed to be proportional to the amplitude of vibration [22–24], that is,

$$V_{cc} = \beta \frac{\alpha_1}{C_p} \hat{u}_{M1}, \quad (19)$$

where β is a coefficient and \hat{u}_{M1} is the vibration amplitude under control.

Substitution of equations (1) and (16)–(19) into equation (5) gives

$$F_{ci} = -\alpha_i V_a = -\alpha_i \left[\frac{\alpha_1}{C_p} u_1(t) + \sum_{j=1}^{\infty} \frac{4}{(2j-1)\pi} \frac{1+\gamma}{1-\gamma} \times \frac{\alpha_1}{C_p} (1+\beta) \hat{u}_{M1} \sin(2j-1) \left(\omega_e t - \varphi_{u1} + \frac{\pi}{2} \right) \right]. \quad (20)$$

The above result indicates that the control force acting on the i th mode, F_{ci} , which is generated by the switched actuator, contains not only the fundamental harmonic, but superharmonic components. If the natural frequency of the i th mode is close to the frequency of $(2j-1)$ th superharmonic components, that is $\omega_{ni} \approx (2j-1)\omega_e$, the mode will be strongly excited. In a structure with dense modal frequencies, this is very likely to happen. The response of the system at superharmonic frequencies will be discussed in the next

where

$$\begin{aligned} \tilde{K}_{S11}^2 &= \frac{\alpha_1^2}{K_{E1} C_p}, \quad K_{D1} = K_{E1} + \frac{\alpha_1^2}{C_p} = K_{E1}(1 + \tilde{K}_{S11}^2), \\ \bar{\omega}_{n1} &= \sqrt{K_{D1}/M_1} \end{aligned} \quad (22)$$

are the squared electromechanical coupling coefficient of the structure, the modal stiffness when the piezoelectric actuator is in open-circuit state, and the angular natural frequency of the first mode with the actuator in open-circuit state, respectively.

The above results give the displacement response when the structure is excited at a non-resonance frequency. In a real structure, the condition $\tilde{K}_{S11}^2 \ll 1$ holds. If the structure is excited at the resonance frequency, then $\omega_e = \bar{\omega}_{n1}$ and the above results are simplified to those obtained in the previous studies [28]. The attenuation is defined as

$$\begin{aligned} A &= 20 \log_{10} \frac{u_{M1}}{\hat{u}_{M1}} \\ &\approx 10 \log_{10} \frac{\left(1 - \left(\frac{\omega_e}{\omega_{n1}} \right)^2 \right)^2 + \left(2\zeta_1 \left(\frac{\omega_e}{\omega_{n1}} \right) + \frac{4}{\pi} \frac{1+\gamma}{1-\gamma} (1+\beta) \tilde{K}_{S11}^2 \right)^2}{\left(1 - \left(\frac{\omega_e}{\omega_{n1}} \right)^2 \right)^2 + \left(2\zeta_1 \left(\frac{\omega_e}{\omega_{n1}} \right) \right)^2}. \end{aligned} \quad (23)$$

subsection. In this subsection, the targeted mode with $i = 1$ is considered.

When $i = 1$, the fundamental harmonic in F_{c1} is the control force for suppression of the vibration excited by the external force. The superharmonic vibrations of the targeted mode excited by the control force F_{c1} are relatively small compared to the fundamental harmonic because the frequencies of the superharmonic forces in F_{c1} are several times larger than the natural frequency of the targeted mode ($(2j-1)\omega_e \gg \omega_{n1}$ with $j \geq 2$) and will be further discussed in the next subsection.

Substitution of F_{e1} , F_{c1} and $u_1(t)$ in equations (6), (9) and (20) into equation (3) by setting i to 1 and solving the amplitude \hat{u}_{M1} and phase $\hat{\varphi}_{u1}$ under control from the resulting equation gives

In the above expression, the approximations $\bar{\omega}_{n1} \approx \omega_{n1}$ and $\tilde{K}_{S11}^2 + 1 \approx 1$ have been used because of the condition $\tilde{K}_{S11}^2 \ll 1$. When $\omega_e = \omega_{n1}$, the above expression for attenuation is simplified to

$$\begin{aligned} A &= 20 \log_{10} \left(1 + \frac{1}{2\zeta_1} \frac{4}{\pi} \frac{1+\gamma}{1-\gamma} (1+\beta) \tilde{K}_{S11}^2 \right) \\ &\approx 20 \log_{10} \left(\frac{1}{2\zeta_1} \frac{4}{\pi} \frac{1+\gamma}{1-\gamma} (1+\beta) \tilde{K}_{S11}^2 \right). \end{aligned} \quad (24)$$

This expression is the same as that obtained in previous studies of SSDV control [26].

$$\left\{ \begin{aligned} \hat{u}_{M1} &= \frac{F_{M1}/K_{D1}}{\sqrt{\left(1 - \left(\frac{\omega_e}{\bar{\omega}_{n1}} \right)^2 \right)^2 + \left(2\zeta_1 \left(\frac{\omega_e}{\bar{\omega}_{n1}} \right) + \frac{4}{\pi} \frac{1+\gamma}{1-\gamma} (1+\beta) \frac{\tilde{K}_{S11}^2}{1+\tilde{K}_{S11}^2} \right)^2}}, \\ \tan \hat{\varphi}_{u1} &= \frac{2\zeta_1 \left(\frac{\omega_e}{\bar{\omega}_{n1}} \right) + \frac{4}{\pi} \frac{1+\gamma}{1-\gamma} (1+\beta) \frac{\tilde{K}_{S11}^2}{1+\tilde{K}_{S11}^2}}{1 - \left(\frac{\omega_e}{\bar{\omega}_{n1}} \right)^2} \end{aligned} \right. \quad (21)$$

2.3. Superharmonic vibration induced by switched actuator voltage

As shown in equation (18), the actuator force includes an infinite number of superharmonic components. Although the amplitude of the superharmonic component of the actuator force decreases as the order, $(2j - 1)$ ($j = 2, 3, \dots$), increases, the higher-order modes can still be effectively excited if their frequencies are sufficiently close. For convenience of analysis, it is assumed that the frequency of the $(2j - 1)$ th superharmonic component, $(2j - 1)\omega_e$, is sufficiently close to the frequency of the i th mode, ω_{ni} , that is, $\omega_{ni} \approx (2j - 1)\omega_e$. By neglecting the other superharmonic components, whose frequencies are far from the resonance frequency of the i th mode, the modal force is approximately expressed as

$$F_{ci} = -\alpha_i \frac{4}{(2j - 1)\pi} \frac{1 + \gamma}{1 - \gamma} \frac{\alpha_1}{C_p} (1 + \beta) \hat{u}_{M1} \times \sin(2j - 1) \left(\omega_e t - \varphi_{u1} + \frac{\pi}{2} \right). \quad (25)$$

The response is assumed to be

$$u_{i(2j-1)}(t) = u_{Mi(2j-1)} \sin[(2j - 1)\omega_e t - \varphi_{ui(2j-1)}]. \quad (26)$$

Substitution of equations (25) and (26) into equation (3) and solutions of $u_{Mi(2j-1)}$ and $\varphi_{ui(2j-1)}$ from the resulting equation yield:

$$u_{Mi(2j-1)} = \frac{\frac{4}{(2j-1)\pi} \frac{1+\gamma}{1-\gamma} (1+\beta) \tilde{K}_{S1i}^2}{\sqrt{\left(1 - \left(\frac{(2j-1)\omega_e}{\omega_{ni}}\right)^2\right)^2 + \left(2\zeta_i \left(\frac{(2j-1)\omega_e}{\omega_{ni}}\right)\right)^2}} \hat{u}_{M1},$$

$$\tan \varphi'_{ui(2j-1)} = \frac{2\zeta_i (2j - 1)\omega_e / \omega_{ni}}{1 - \left(\frac{(2j - 1)\omega_e}{\omega_{ni}}\right)^2} + \pi,$$

$$\varphi_{ui(2j-1)} = (2j - 1) \left(\varphi_{u1} - \frac{\pi}{2} \right) + \varphi'_{ui(2j-1)}, \quad (27)$$

where $\tilde{K}_{S1i}^2 = \frac{\alpha_1 \alpha_i}{K_{Ei} C_p}$. The first expression in equation (27) gives the ratio between the amplitude of the $(2j - 1)$ th superharmonic in the i th mode and the controlled amplitude of the targeted mode (the first mode in this case), which is the factor before \hat{u}_{M1} on the right-hand side of the expression. When the ratio $u_{Mi(2j-1)}/\hat{u}_{M1}$ is smaller than 0.1, it may be thought that the excited vibration is not significant.

First, the special case with $i = 1$ and $(2j - 1) = 3$, the third superharmonic vibration of the targeted mode, is considered. If $\omega_e = \omega_{n1}$ and the damping ratio is sufficiently small, then the amplitude can be approximately expressed in the following form:

$$u_{M1(3)}/\hat{u}_{M1} = \frac{1}{24} \cdot \frac{4}{\pi} \frac{1 + \gamma}{1 - \gamma} (1 + \beta) \tilde{K}_{S11}^2. \quad (28)$$

This expression gives the ratio between $u_{M1(3)}$ and \hat{u}_{M1} . As shown in equation (24), the control performance of the fundamental harmonic mainly depends on the factor $\frac{4}{\pi} \frac{1 + \gamma}{1 - \gamma} (1 + \beta) \tilde{K}_{S11}^2$, which also directly affects the control performance, as shown in equation (28). As shown in the

previous studies, the vibration attenuation of SSDV is usually 20–35 dB [27, 28, 33]. This means that the factor is usually smaller than 1 if the damping ratio of the mode is assumed to be $\zeta_i = 0.01$. Hence, the third harmonic of the first mode is at least one-order smaller than the fundamental harmonic and is negligible.

Next, another special case of $\omega_{ni} = (2j - 1)\omega_e$ with a given pair of i and j is considered. The ratio $u_{Mi(2j-1)}/u_{M1}$ can be expressed in the following form:

$$u_{Mi(2j-1)}/\hat{u}_{M1} = \frac{1}{(2j - 1)} \cdot \frac{1}{2\zeta_i} \cdot \frac{4}{\pi} \frac{1 + \gamma}{1 - \gamma} (1 + \beta) \tilde{K}_{S1i}^2. \quad (29)$$

If $\zeta_i = \zeta_1$ and $\tilde{K}_{S1i} = \tilde{K}_{S11}$, then the term $\frac{1}{2\zeta_i} \cdot \frac{4}{\pi} \frac{1 + \gamma}{1 - \gamma} (1 + \beta) \tilde{K}_{S1i}^2$ is the same as that in equation (24). Its value usually ranges from 10–50, depending on the required control performance. This indicates that the amplitude of superharmonic vibration, $u_{Mi(2j-1)}$, can be much larger than the controlled amplitude of the targeted mode, \hat{u}_{M1} , if the condition $\omega_{ni} = (2j - 1)\omega_e$ is satisfied. In a practical structural system, this condition is not exactly satisfied, but it is highly possible that it is approximately satisfied.

As an example, a cantilever beam is considered. Theoretically, the relationship $\omega_{n2} = 6.2764\omega_{n1}$ holds for a cantilever beam. If the excitation frequency satisfies $\omega_e = 0.8966\omega_{n1}$, that is, just a little lower than the first resonance frequency, then there exists $7\omega_e \approx \omega_{n2}$. Letting $i = 2$ and $(2j - 1) = 7$ in equation (29), we obtain

$$u_{M2,7}/\hat{u}_{M1} = \frac{1}{7} \cdot \frac{1}{2\zeta_2} \cdot \frac{4}{\pi} \frac{1 + \gamma}{1 - \gamma} (1 + \beta) \tilde{K}_{S12}^2. \quad (30)$$

Since $\frac{1}{2\zeta_2} \cdot \frac{4}{\pi} \frac{1 + \gamma}{1 - \gamma} (1 + \beta) \tilde{K}_{S12}^2$ approximately ranges from 10–50, the ratio $u_{M2,7}/\hat{u}_{M1}$ can be as large as seven. Therefore, the suppression of superharmonic vibration is very important in semi-active control.

3. Reduction of superharmonic components by increasing voltage inversion time

3.1. Analysis of the switched voltage with finite inversion time

In the above analysis, the voltage inversion time is assumed to be infinitesimal and the switched voltage is assumed to have rectangular waveform. In this section, the voltage inversion time is assumed to be finite. If the period of the LC circuit for voltage inversion is τ_c , the switch circuit is closed at the displacement extrema and kept closed for a duration of $\tau_c/2$ for voltage inversion, as shown in figure 3. Hence, the inversion time is $\tau_c/2$, half the period of the LC circuit. A new parameter, called switching time ratio, is defined as

$$\mu = \frac{\tau_c}{2\tau_{sw}}. \quad (31)$$

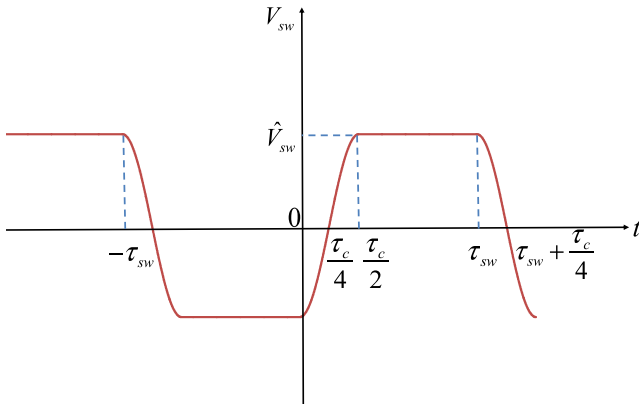


Figure 3. Switched voltage.

Obviously, switching time ratio μ can be changed from 0 to 1. When μ is 0, the inversion time is infinitesimal. When μ equals to 1, the switched voltage becomes an ideal sinusoidal waveform.

The same expression of excitation and displacement response shown in equation (6) is assumed in the following analysis. When the voltage is switched at the displacement extrema, the switching points are also the same as those in equation (15). The waveform of $V_{sw}(t)$ is plotted in figure 3 for $\varphi'_{u1} = 0$. For convenience of analysis, a shift of the time axis is carried out. The new time is defined as

$$t' = t - \frac{\varphi'_{u1}}{\omega_e} - \frac{\tau_c}{4} = t - \frac{\varphi'_{u1}}{\omega_e} - \frac{\mu\pi}{2\omega_e}. \quad (32)$$

Obviously, the switched voltage in the new time domain, $V_{sw}(t')$ is an odd function. The switched voltage is expressed in the following form:

$$V_{sw}(t') = \hat{V}_{sw} S'_c(t'), \quad (33)$$

where \hat{V}_{sw} is the amplitude of V_{sw} given in equation (12), $S'_c(t')$ is the switch function in the new time domain. The switch function can be expressed in the following form:

$$S'_c(t') = \begin{cases} \sin\left(\omega_c t' + \frac{\pi}{\mu} + \pi\right) & 2\tau_{sw}k' - \tau_{sw} < t' < 2\tau_{sw}k' - \tau_{sw} + \frac{\tau_c}{4} \\ -1 & 2\tau_{sw}k' - \tau_{sw} + \frac{\tau_c}{4} < t' < 2\tau_{sw}k' - \frac{\tau_c}{4} \\ \sin(\omega_c t') & 2\tau_{sw}k' - \frac{\tau_c}{4} < t' < 2\tau_{sw}k' + \frac{\tau_c}{4} \\ 1 & 2\tau_{sw}k' + \frac{\tau_c}{4} < t' < 2\tau_{sw}k' + \tau_{sw} - \frac{\tau_c}{4} \\ \sin\left(\omega_c t' - \frac{\pi}{\mu} + \pi\right) & 2\tau_{sw}k' + \tau_{sw} - \frac{\tau_c}{4} < t' < 2\tau_{sw}k' + \tau_{sw} \end{cases}, \quad (34)$$

where k' is an integer and

$$\omega_c = \frac{2\pi}{\tau_c}, \quad (35)$$

is the angular frequency of the switch circuit.

The switched voltage is periodic. Its frequency is the same as the harmonic vibration used for switch control. The k th-order harmonic of the switched voltage can be expressed as

$$V_{sw,k} = \frac{4\hat{V}_{sw}}{k\pi} \frac{1}{1 - (k\mu)^2} \cos k\mu \frac{\pi}{2} \sin k\left(\omega_e t - \varphi'_{u1} - \mu \frac{\pi}{2}\right). \quad (36)$$

This expression indicates that the phase delay is induced by the voltage inversion time.

The amplitude of superharmonic components in the switched voltage is normalized as follows:

$$\bar{V}_{sw,k} = \frac{b_k^{sw}}{\hat{V}_{sw}}. \quad (37)$$

The normalized amplitude of the superharmonic voltages is plotted as a function of the order k in figure 4 for $0 < k < 21$, with the frequency ratio μ as a parameter taking values of 0, 0.2, 0.4, 0.6, 0.8 and 0.99, respectively. In order to more clearly display the results, the normalized amplitudes are plotted as a function of μ with k equal to 1, 3 and 5 in figure 5 and with k equal to 7, 9 and 11 in figure 6. When $\mu = 0$, the voltage inversion time is infinitesimal and the switched voltage has a rectangular waveform. When $\mu = 0.99$, the voltage inversion time is almost half the period of mechanical vibration. The generated voltage on PZT becomes a harmonic waveform.

Since the actuator force is directly proportional to the actuator voltage, it is very important to reduce the superharmonic components of the switch voltage. When the voltage is switched in infinitesimal time ($\mu = 0$), the normalized voltage amplitude of the superharmonic components is in inverse proportion to its order. Although the normalized amplitude decreases as the order increases, strong superharmonic vibration can still be excited for the first several superharmonic components if their frequencies are close enough to the natural frequency of certain structural modes. Hence, it is very important for further reducing the normalized amplitude of the superharmonic voltages by increasing the inversion time. One effective method is to increase the value of the inductor. Obviously, the normalized amplitude of the

superharmonic voltages decreases as μ increases from 0 to 1. However, the rate of decrease is different for different superharmonic components. An inversion time of $\mu = 0.5$ is enough for all the superharmonic $k \geq 5$, but an inversion time of $\mu \geq 0.9$ is necessary for the superharmonic $k = 3$. The

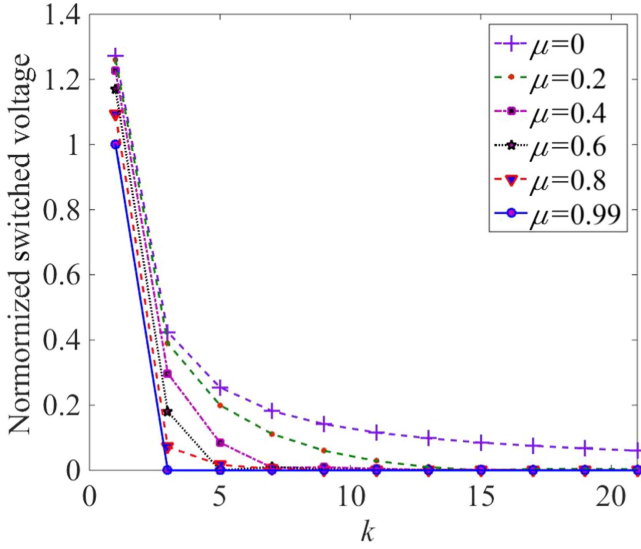


Figure 4. Normalized switched voltages as a function of k .

normalized amplitude of the fundamental harmonic is $4/\pi$ for $\mu = 0$ and 1 for $\mu = 1$. This means that although the normalized amplitude of the fundamental harmonic decreases as μ increases, the percentage decrease is about 21%, not as significant as for the superharmonic components.

3.2. Influence of voltage inversion time on control performance

The voltage inversion time does not only affect the amplitude of fundamental harmonic voltage, but its phase. Hence, it is important to investigate its influence on the control performance. According to equations (11), (18) and (36), the force generated by the piezoelectric actuator and acting on the i th mode can be expressed as

$$\begin{aligned}
 F_{ci} = -\alpha_i V_a = -\alpha_i \left[\frac{\alpha_1}{C_p} u_1(t) + \sum_{j=1}^{\infty} \left\{ u_{M1} \frac{4}{(2j-1)\pi} \right. \right. \\
 \times \frac{1 + \gamma \alpha_1}{1 - \gamma C_p} (1 + \beta) \cdot \frac{1}{1 - ((2j-1)\mu)^2} \cos \\
 \times \left((2j-1)\mu \frac{\pi}{2} \right) \sin(2j-1) \\
 \left. \left. \times \left(\omega_e t - \varphi_{u1} + \frac{\pi}{2} - \mu \frac{\pi}{2} \right) \right\} \right]. \quad (38)
 \end{aligned}$$

Obviously, the phase delay is induced when μ is greater than 0.

In order to investigate the control performance of the targeted mode, only the fundamental harmonic in the control

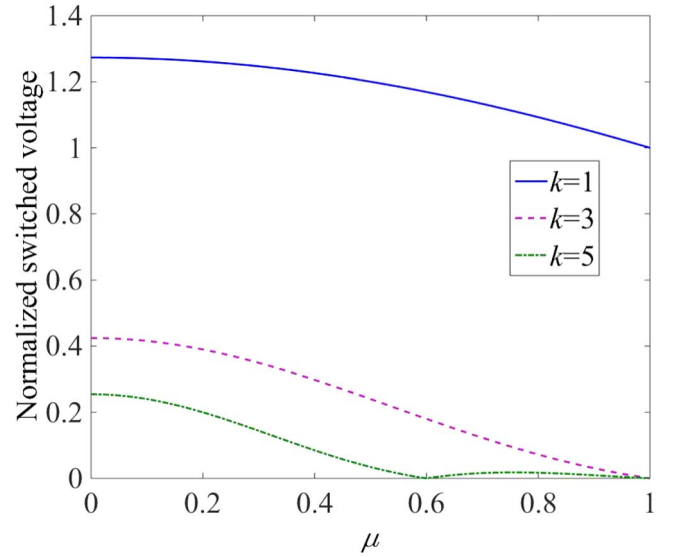


Figure 5. Normalized switched voltages as a function of μ .

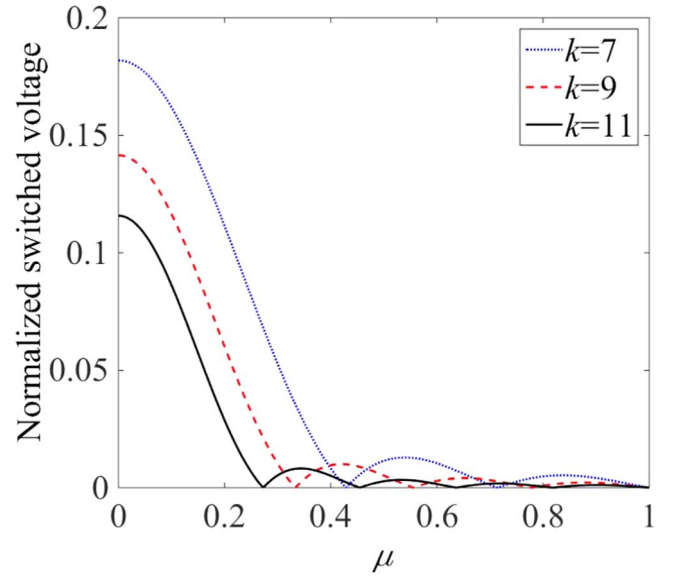


Figure 6. Normalized switched voltages as a function of μ .

force in equation (38) is considered by neglecting the superharmonic components.

The submission of F_{e1} , F_{c1} and $u_1(t)$ in equations (6), (8) and (38) into equation (3) by setting i to 1 and solving \hat{u}_{M1} and $\hat{\varphi}_{u1}$, the amplitude and phase angle under control, from the resulting equation give

$$\begin{cases} \hat{u}_{M1} = \frac{F_{M1}/K_{D1}}{\sqrt{\left[1 - \left(\frac{\omega_e}{\omega_{n1}} \right)^2 + \kappa_{11} \sin \frac{\mu\pi}{2} \right]^2 + \left[2\zeta_1 \left(\frac{\omega_e}{\omega_{n1}} \right) + \kappa_{11} \cos \frac{\mu\pi}{2} \right]^2}} \\ \tan \hat{\varphi}_{u1} = \frac{2\zeta_1 \left(\frac{\omega_e}{\omega_{n1}} \right) + \kappa_{11} \cos \frac{\mu\pi}{2}}{1 - \left(\frac{\omega_e}{\omega_{n1}} \right)^2 + \kappa_{11} \sin \frac{\mu\pi}{2}} \end{cases}, \quad (39)$$

where

$$\kappa_{11} = \frac{4}{\pi} \frac{1 + \gamma}{1 - \gamma} (1 + \beta) \frac{1}{1 - \mu^2} \cos \mu \frac{\pi}{2} \frac{\tilde{K}_{S11}^2}{1 + \tilde{K}_{S11}^2}. \quad (40)$$

The denominator in the expression is zero when $\mu = 1$, but its limit exists when μ approaches 1. The value of κ_{11} at $\mu = 1$ is defined by the limit, which is

$$\kappa_{11} = \frac{1 + \gamma}{1 - \gamma} (1 + \beta) \frac{\tilde{K}_{S11}^2}{1 + \tilde{K}_{S11}^2}. \quad (41)$$

Equation (39) indicates that due to the phase delay in the actuator force it does not only influence the damping of the structure, but also its stiffness. If $\omega_e = \bar{\omega}_{n1}$ and $\mu = 1$, then there exists approximately

$$\hat{u}_{M1} \approx \frac{1}{\kappa_{11}} \frac{F_{M1}}{K_{D1}}, \quad \hat{\varphi}_{u1} \approx 0, \quad (42)$$

because $\zeta_1 \ll \kappa_{11}$. This means that the displacement is almost in phase with the external excitation.

The attenuation is defined as

$$A = 20 \log_{10} \frac{u_{M1}}{\hat{u}_{M1}} \approx 10 \log_{10} \frac{\left[1 - \left(\frac{\omega_e}{\bar{\omega}_{n1}} \right)^2 + \kappa_{11} \sin \frac{\mu\pi}{2} \right]^2 + \left[2\zeta_1 \left(\frac{\omega_e}{\bar{\omega}_{n1}} \right) + \kappa_{11} \cos \frac{\mu\pi}{2} \right]^2}{\left(1 - \left(\frac{\omega_e}{\omega_{n1}} \right)^2 \right)^2 + \left(2\zeta_1 \left(\frac{\omega_e}{\omega_{n1}} \right) \right)^2}. \quad (43)$$

The same approximations as those used in equation (24) have been used in the above equation. In the case that $\omega_e = \bar{\omega}_{n1}$ and $\mu = 1$, the attenuation can be approximately expressed as

$$A = 10 \log_{10} \left[1 + \left(\frac{1}{2\zeta_1} \frac{1 + \gamma}{1 - \gamma} (1 + \beta) \frac{\tilde{K}_{S11}^2}{1 + \tilde{K}_{S11}^2} \right)^2 \right] \approx 20 \log_{10} \left(\frac{1}{2\zeta_1} \frac{1 + \gamma}{1 - \gamma} (1 + \beta) \tilde{K}_{S11}^2 \right). \quad (44)$$

Comparison of equations (24) and (44) indicates that the attenuation of the targeted mode is weakened, but it is only reduced by $20 \log_{10}(4/\pi) = 2$ dB for the same values of system parameters ζ_1 , γ , β and \tilde{K}_{S11} when the switching time ratio μ is raised from 0 to 1.

3.3. Reduction of the superharmonic vibration

Similar to the analysis in section 2.3, the vibration of the i th mode excited by the k th superharmonic component in the actuator voltage is considered. The modal force acting on i th mode due to k th ($k = 2j - 1$) superharmonic components of

actuator voltage is

$$F_{ci} = -\alpha_i \hat{u}_{M1} \frac{4}{(2j-1)\pi} \frac{1 + \gamma}{1 - \gamma} \frac{\alpha_1}{C_p} (1 + \beta) \cdot \frac{1}{1 - ((2j-1)\mu)^2} \cos \left((2j-1)\mu \frac{\pi}{2} \right) \times \sin(2j-1) \left(\omega_e t - \varphi_{u1} + \frac{\pi}{2} - \mu \frac{\pi}{2} \right) = -\kappa_{1i(2j-1)} K_{Ei} \hat{u}_{M1} \sin(2j-1) \times \left(\omega_e t - \varphi_{u1} + \frac{\pi}{2} - \mu \frac{\pi}{2} \right), \quad (45)$$

where

$$\kappa_{1i(2j-1)} = \frac{4}{(2j-1)\pi} \frac{1 + \gamma}{1 - \gamma} \frac{\alpha_1 \alpha_i}{K_{Ei} C_p} (1 + \beta) \times \frac{1}{1 - ((2j-1)\mu)^2} \cos \left((2j-1)\mu \frac{\pi}{2} \right). \quad (46)$$

The response with finite inversion time is assumed to be

$$\tilde{u}_{i(2j-1)}(t) = \tilde{u}_{Mi(2j-1)} \sin[(2j-1)\omega_e t - \tilde{\varphi}_{ui(2j-1)}]. \quad (47)$$

Substitution of equations (45) and (47) into equation (3) and solution of $u_{Mi(2j-1)}$ and $\varphi_{ui(2j-1)}$ from the resulting equation yield

$$\tilde{u}_{Mi(2j-1)} = \frac{\kappa_{1i(2j-1)} \hat{u}_{M1}}{\sqrt{\left(1 - \left(\frac{(2j-1)\omega_e}{\omega_{ni}} \right)^2 \right)^2 + \left(2\zeta_i \left(\frac{(2j-1)\omega_e}{\omega_{ni}} \right) \right)^2}} \tan \tilde{\varphi}'_{ui(2j-1)} = \frac{2\zeta_i (2j-1) \omega_e / \omega_{ni}}{1 - ((2j-1)\omega_e / \omega_{ni})^2} + \pi \tilde{\varphi}_{ui(2j-1)} = (2j-1) \left(\varphi_{u1} - \frac{\pi}{2} + \mu \frac{\pi}{2} \right) + \tilde{\varphi}'_{ui(2j-1)}. \quad (48)$$

In order to evaluate the reduction of the superharmonic components of vibration, an attenuation index is defined as follows:

$$A_{i(2j-1)} = 20 \log_{10} \frac{u_{Mi(2j-1)}}{|\tilde{u}_{Mi(2j-1)}|} = 20 \log_{10} \left| \frac{1 - ((2j-1)\mu)^2}{\cos((2j-1)\mu\pi/2)} \right|. \quad (49)$$

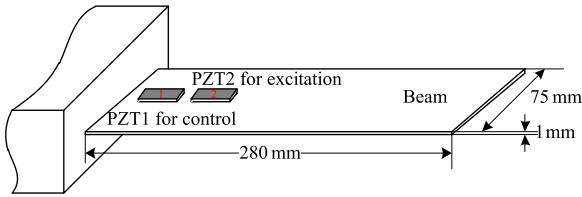


Figure 7. Schematic representation of the beam.

The larger the value of $A_{i(2j-1)}$ is, the better the performance in the reduction of the superharmonic components will be. The attenuation index depends only on the order of the superharmonic components. It is independent of the order of the vibration mode. Because $A_{i(2j-1)}$ is infinity for any value of j when $\mu = 1$, all superharmonic components of vibration are completely canceled. This agrees well with the results of the superharmonic force components in figures 4–6 that all the superharmonic components are zero at $\mu = 1$.

4. Experimental validation and discussion

4.1. Experimental system

For experimental validation of the method proposed above to reduce the superharmonic vibrations, semi-active control of a cantilever aluminum beam was employed. The length, width and thickness of the beam, as shown in figure 7, are 280, 75 and 1 mm, respectively. The two piezoelectric patches, PZT1 and PZT2, are bonded onto the surface near the clamped end, where the maximum strain is induced. The inherent capacitance of both of the piezoelectric actuators is 3.8 pF. The size of the piezoelectric patches is $30 \times 30 \times 0.2$ mm. They are polarized in the thickness direction. PZT2 was used to excite the vibration of the beam, while PZT1 was used to control the vibration. The natural frequencies of the first two modes are 10.41 and 57.1 Hz, respectively, that is, there exists $5.49\omega_{n1} \approx \omega_{n2}$. Due to the influence of the bonded piezoelectric elements and the imperfect boundary conditions, the frequency ratio of the first two modes is different to the theoretical value. The displacement at the free end of the beam was measured by a laser displacement sensor and the signal was used for switch control in the shunt circuit. The schematic chart of the enhanced SSDV control system is shown in figure 8, in which the voltage source is proportional to the vibration amplitude, shown as equation (19).

The beam was excited at the first resonance frequency 10.41 Hz. Inductors of 0.3, 4.4, 9.6, 16.7 and 24.8 H were used in enhanced SSDV control to change the inversion time of the voltage by the shunt circuit. Corresponding to these values of inductance, the switching time ratio defined in equation (31) is 7%, 24%, 38%, 50% and 61%, respectively. The voltage coefficient β was set as 15. In experiments, it is impossible to realize zero inversion time.

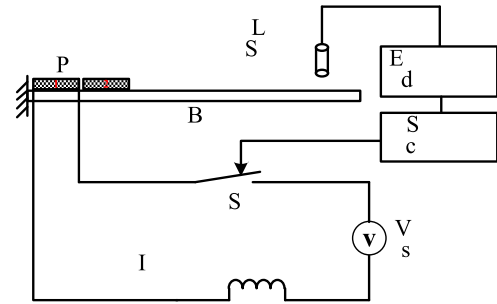


Figure 8. Experimental setup.

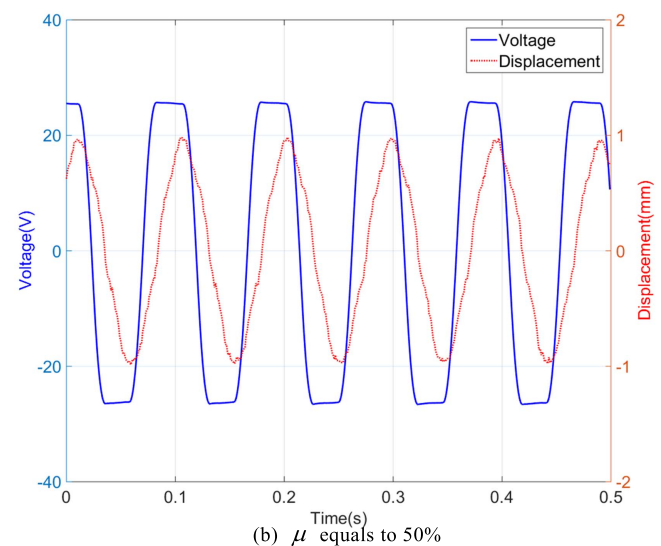
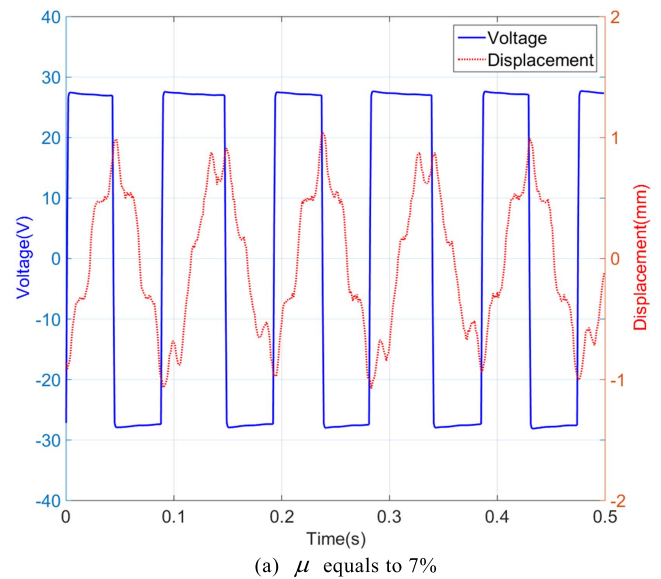


Figure 9. Output voltage of piezoelectric element and displacement of the beam.

4.2. Experimental results and discussion

The actuator voltage on the PZT and the displacement of the beam in two typical cases, where $\mu = 7\%$ and $\mu = 50\%$, are shown in figure 9. When the inductance is 0.3 H ($\mu = 7\%$), the inversion time is very short and the voltage waveform

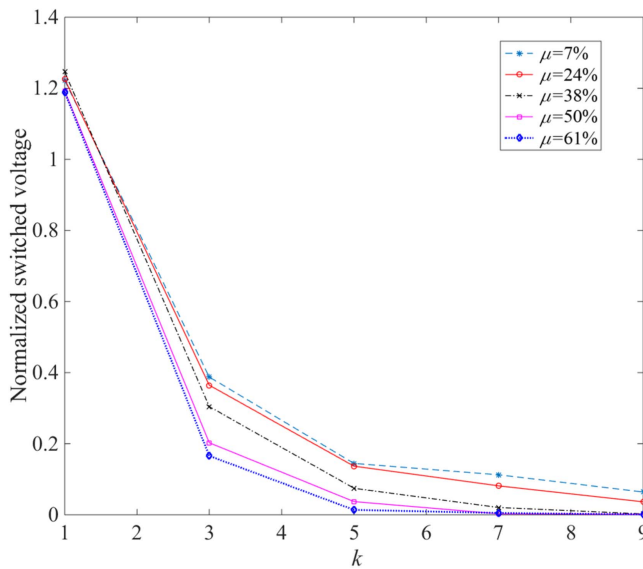


Figure 10. Experimental results of the normalized switched voltages as a function of k .

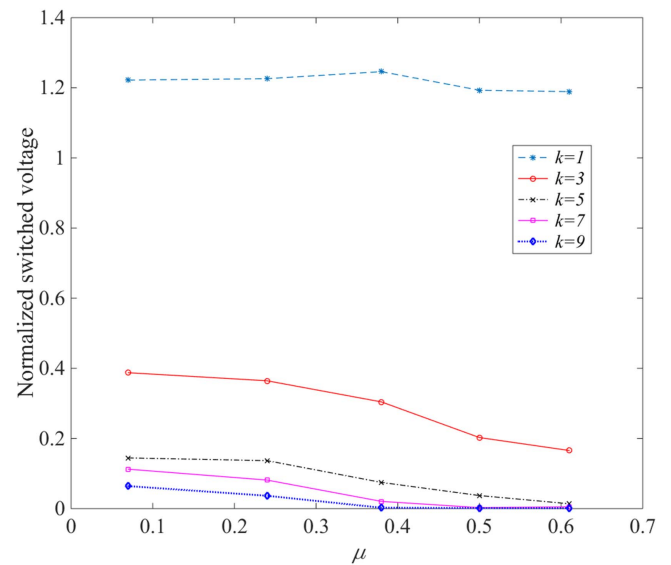


Figure 11. Experimental results of the normalized switched voltages as a function of μ .

looks almost rectangular. The 5th superharmonic vibration was significantly excited because the frequency of the 5th superharmonic is very close to the natural frequency of the 2nd mode of the beam. The slight decrease at the plateau of the voltage waveform is due to circuit leakage [6]. It can also be observed that the voltage is not switched exactly at the displacement extrema of the first mode due to the influences of the second mode. Actually, the two modes coupled in this case, as was discussed in the previous studies [30]. When an inductor of 16.7 H ($\mu = 50\%$) was used, the width of the plateau in the voltage waveform is 50% of that in the ideal switching condition. The amplitude of the 5th superharmonic has been significantly reduced.

In order to validate the theoretical results of the switched voltage and control performance, Fourier transform was used to extract the amplitude of the superharmonic components of the actuator voltage and normalized by the voltage amplitude at the plateau, which corresponds to the V_{sw} in equation (12). The switched voltages of k th-order harmonic ($k = 1, 3, 5, 7$ and 9) when μ equals to 7%, 24%, 38%, 50% and 61% are plotted in figure 10. Although there are some differences between the experimental and theoretical results, as shown in figure 4, their trends are very similar. There are many factors that may affect the experimental results, such as, errors in inductor values, measurement noise in experiments, the delay of switching action, etc. The results of the experiments further confirm that the voltage of the high-order harmonic component can be effectively suppressed by increasing the inversion time of the voltage by the shunt circuit. When μ is over 0.5, the 5th harmonic component is very small. The amplitudes of normalized switched voltage are plotted as a function of μ in figure 11 with parameter k equal to 1, 3, 5, 7 and 9, respectively. These results are also very similar to the theoretical results shown in figures 5 and 6.

Figure 12 shows the amplitude of the targeted mode and the vibration excited by the fifth superharmonic under

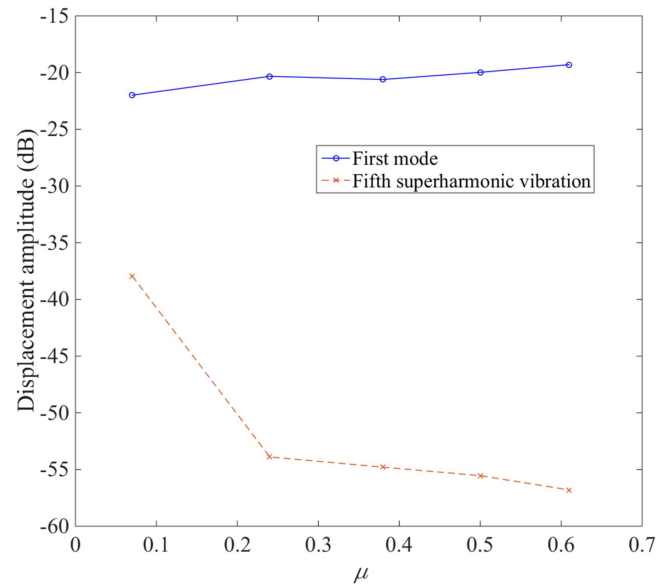


Figure 12. Spectrum of the displacement of the beam.

enhanced SSDV control with parameter μ equal to 7%, 24%, 38%, 50% and 61%, respectively. The vibration amplitude of the first mode increases slightly with the increase of inversion time. There is only 2.69 dB reduction when the switching time ratio was increased from $\mu = 7\%$ to $\mu = 61\%$. However, the amplitude of the fifth superharmonic vibration was reduced significantly when the switching time ratio was raised. The sudden reduction of the fifth superharmonic as μ is increased from 7% to 24%, was due to decoupling between the first and second modes. As shown in figure 9(a), the amplitude of the fifth superharmonic is large enough to affect the switching point in the displacement response. That is, the switching point is determined by the vibration of both the first and second modes and the actuator voltage is not uniformly

switched, so that the switching frequency contains two components. Hence, the first and second modes are coupled [30]. When the amplitude of the fifth superharmonic is reduced by increasing the switching time ratio, decoupling between the first two modes is achieved and the vibration amplitude of the second mode can be significantly reduced.




5. Conclusion

In the classical SSD control, smaller inductance, which makes the inversion time of the LC circuit shorter, is considered better for control performance. But it results in a rectangular waveform of actuator voltage on the piezoelectric element. The rectangular waveform gives high control voltage for the targeted vibration mode, consequently yielding high control performance, but it also contains rich superharmonic components, which may excite undesired high-order modes. When the frequency of a certain superharmonic is sufficiently close to the natural frequency of a certain mode of the structure, the amplitude of the excited high-order mode may reach a nonnegligible level, especially when coupling occurs between the targeted mode and excited high-order mode. Therefore, reduction of superharmonic components in the switched voltage is very important in semi-active SSDV control. In this study, a new method to reduce the superharmonic components in the switched voltage by increasing the inversion time in the LC circuit has proposed. The general expressions of the switched voltage on the piezoelectric actuator under different inversion time conditions were derived. Based on its periodicity in steady-state control, the harmonic components of the actuator voltage were derived using Fourier series expansions. The vibration of high-order modes excited by superharmonic components of the switched actuator voltage has also been solved. An experimental setup of a cantilever beam was built to validate the theoretical results. The results show that the control performance of the fundamental harmonic vibration was only slightly affected by increasing the switching time, but the superharmonic vibration excited by the actuator voltage was greatly reduced. The theoretical and experimental results verified the advantages of the proposed method by increasing the inversion time of the LC circuit in SSDV control. This method can further extend the application of SSDV control in practical structures where superharmonic vibrations are critically harmful.

Acknowledgments

This research is supported by the National Natural Science Foundation of China under Grants 11532006, 51775267 and 51375228, the Aeronautical Science Fund under Grant 20161552014, the Fundamental Research Funds for the Central Universities under Grant NE2015001, and PAPD.

ORCID iDs

Hongli Ji  <https://orcid.org/0000-0002-7109-9971>
 Yipeng Wu  <https://orcid.org/0000-0002-7328-3836>
 Li Cheng  <https://orcid.org/0000-0001-6110-8099>

References

- [1] Forward R L and Swigert C J 1981 Electronic damping of orthogonal bending modes in a cylindrical mast-experiment *J. Spacecr. Rockets* **18** 5–10
- [2] Mikułowski G, Fournier M, Porchez T, Belly C and Claeysen F 2016 Semi-passive vibration control technique via shunting of amplified piezoelectric actuators *ACTUATOR 2016, 15th Int. Conf. on New Actuators (Bremen, Germany)* pp 13–5
- [3] Richard C et al 1998 Semi-passive damping using continuous switching of a piezoelectric device *SPIE Smart Structures and Materials Conf.: Passive Damping and Isolation* pp 104–11
- [4] Tang W et al 2017 Experimental comparisons of two detection methods for semi-passive piezoelectric structural damping *J. Vib. Eng. Technol.* **5** 367–79
- [5] Liu J et al 2017 Dynamic characteristics of the blisk with synchronized switch damping based on negative capacitor *Mech. Syst. Signal Process.* **95** 425–45
- [6] Ji H et al 2016 Semi-active vibration control based on unsymmetrical synchronized switch damping: Analysis and experimental validation of control performance *J. Sound Vib.* **370** 1–22
- [7] Cherif A et al 2016 Multimodal vibration damping using energy transfer *Opt. Quantum Electron.* **48** 283
- [8] Qureshi E M, Shen X and Chen J J 2014 Vibration control laws via shunted piezoelectric transducers: a review *Int. J. Aeronaut. Space Sci.* **15** 1–19
- [9] Formosa F et al 2013 Piezoelectric vibration energy harvesting by optimized synchronous electric charge extraction *J. Intell. Mater. Syst. Struct.* **24** 1445–58
- [10] Wang Y and Inman D J 2013 Experimental validation for a multifunctional wing spar with sensing, harvesting, and gust alleviation capabilities *IEEE/ASME Trans. Mechatronics* **18** 1289–99
- [11] Kamiya K A new approach for piezoelectric switched shunt damping on inductance *ASME. Int. Design Engineering Technical Conf. and Computers and Information in Engineering Conf., Volume 8: 27th Conf. on Mechanical Vibration and Noise V008T13A033* (<https://doi.org/10.1115/DETC2015-46435>)
- [12] Liang J, Chung S H and Liao W H 2014 Dielectric loss against piezoelectric power harvesting *Smart Mater. Struct.* **23** 092001
- [13] Yan B et al 2017 Self-sensing electromagnetic transducer for vibration control of space antenna reflector *IEEE/ASME Trans. Mechatronics* **22** 1944–51
- [14] Bao B and Tang W 2017 Semi-active vibration control featuring a self-sensing SSDV approach *Measurement* **104** 192–203
- [15] Kelley C R and Kauffman J L 2017 Optimal switch timing for piezoelectric-based semi-active vibration reduction techniques *J. Intell. Mater. Syst. Struct.* **28** 2275–85
- [16] Guyomar D and Lallart M 2011 Switching loss reduction in nonlinear piezoelectric conversion under pulsed loading *IEEE Trans. Ultrason. Ferroelectr. Freq. Control* **58** 494–502
- [17] Qiu Z et al 2016 A vision-based vibration sensing and active control for a piezoelectric flexible cantilever plate *J. Vib. Control* **22** 1320–37

- [18] Lallart M *et al* 2013 Electromechanical semi-passive nonlinear tuned mass damper for efficient vibration damping *J. Sound Vib.* **332** 5696–709
- [19] Guyomar D, Richard C and Petit L 2001 Non-linear system for vibration damping *142th Meeting of Acoustical Society of America (Fort Lauderdale, USA)*
- [20] Makihara K, Onoda J and Minesugi K 2007 A self-sensing method for switching vibration suppression with a piezoelectric actuator *Smart Mater. Struct.* **16** 455–61
- [21] Lefeuvre E, Badel A, Petit L, Richard C and Guyomar D 2006 Semi-passive piezoelectric structural damping by synchronized switching on voltage sources *J. Intell. Mater. Syst. Struct.* **17** 653–60
- [22] Badel A, Sebald G, Guyomar D, Lallart M, Lefeuvre E, Richard C and Qiu J H 2006 Piezoelectric vibration control by synchronized switching on adaptive voltage sources: towards wideband semi-active damping *J. Acoust. Soc. Am.* **119** 2815–25
- [23] Ji H L, Qiu J H, Badel A and Zhu K J 2009 Semi-active vibration control of a composite beam using an adaptive SSDV approach *J. Intell. Mater. Syst. Struct.* **20** 401–12
- [24] Ji H L, Qiu J H, Badel A, Chen Y S and Zhu K J 2009 Semi-active vibration control of a composite beam by adaptive synchronized switching on voltage sources based on LMS algorithm *J. Intell. Mater. Syst. Struct.* **20** 939–47
- [25] Khodayari A, Ahmadi A and Mohammadi S 2011 On physical realization of the wireless semi active real time vibration control based on signal statistical behavior *Sensors Actuators A* **167** 102–9
- [26] Mokrani B, Rodrigues G, Ioan B, Bastaits R and Preumont A 2012 Synchronized switch damping on inductor and negative capacitance *J. Intell. Mater. Syst. Struct.* **23** 2065–75
- [27] Ji H, Qiu J, Cheng J and Inman D 2011 Application of a negative capacitance circuit in synchronized switch damping techniques for vibration suppression *J. Vib. Acoust.* **133** 041015
- [28] Ji H, Qiu J and Guyomar D 2010 Influences of switching phase and frequency of voltage on piezoelectric actuator upon vibration damping effect *Smart Mater. Struct.* **20** 015008 16
- [29] Guyomar D, Richard C and Mohammadi S 2007 Semi-passive random vibration control based on statistics *J. Sound Vib.* **307** 818–33
- [30] Ji H L, Qiu J H, Zhu K J and Badel A 2010 Two-mode vibration control using nonlinear synchronized switching damping based on the maximization of converted energy *J. Sound Vib.* **329** 2751–67
- [31] Chérif A, Richard C, Guyomar D, Belkhiat S and Meddad M 2012 Simulation of multimodal vibration damping of a plate structure using a modal SSDI-Max technique *J. Intell. Mater. Syst. Struct.* **23** 675–89
- [32] Ji H, Cheng L, Qiu J and Nie H 2014 Semi-active noise suppression based on SSD technique using piezoelectric elements (Melbourne, Australia) pp 16–9
- [33] Ji H, Qiu J, Xia P and Inman D 2012 Coupling analysis of energy conversion in multi-mode vibration structural control using synchronized switch damping method *Smart Mater. Struct.* **21** 015013 1–16 (16pp)